

# Optics Letters

## Ultralow 0.034 dB/m loss wafer-scale integrated photonics realizing 720 million $Q$ and 380 $\mu$ W threshold Brillouin lasing

KAIKAI LIU,<sup>1</sup>  NAIJUN JIN,<sup>2</sup> HAOTIAN CHENG,<sup>2</sup> NITESH CHAUHAN,<sup>1</sup> MATTHEW W. PUCKETT,<sup>3</sup> KARL D. NELSON,<sup>3</sup> RYAN O. BEHUNIN,<sup>4,5</sup> PETER T. RAKICH,<sup>2</sup> AND DANIEL J. BLUMENTHAL<sup>1,\*</sup> 

<sup>1</sup>Department of Electrical and Computer Engineering, University of California Santa Barbara, Santa Barbara, California, USA

<sup>2</sup>Department of Applied Physics, Yale University, New Haven, Connecticut, USA

<sup>3</sup>Honeywell International, Phoenix, Arizona, USA

<sup>4</sup>Department of Applied Physics and Materials Science, Northern Arizona University, Flagstaff, Arizona, USA

<sup>5</sup>Center for Materials Interfaces in Research and Applications (iMIRA!), Northern Arizona University, Flagstaff, Arizona, USA

\*Corresponding author: danb@ucsb.edu

Received 26 January 2022; accepted 18 February 2022; posted 23 February 2022; published 31 March 2022

We demonstrate 0.034 dB/m loss waveguides in a 200-mm wafer-scale, silicon nitride ( $\text{Si}_3\text{N}_4$ ) CMOS-foundry-compatible integration platform. We fabricate resonators that measure up to a 720 million intrinsic  $Q$  resonator at 1615 nm wavelength with a 258 kHz intrinsic linewidth. This resonator is used to realize a Brillouin laser with an energy-efficient 380  $\mu$ W threshold power. The performance is achieved by reducing scattering losses through a combination of single-mode TM waveguide design and an etched blanket-layer low-pressure chemical vapor deposition (LPCVD) 80 nm  $\text{Si}_3\text{N}_4$  waveguide core combined with thermal oxide lower and tetraethoxysilane plasma-enhanced chemical vapor deposition (TEOS-PECVD) upper oxide cladding. This level of performance will enable photon preservation and energy-efficient generation of the spectrally pure light needed for photonic integration of a wide range of future precision scientific applications, including quantum, precision metrology, and optical atomic clocks. © 2022 Optica Publishing Group

<https://doi.org/10.1364/OL.454392>

Ultralow optical losses are essential for preserving photons and generating spectrally pure light in a wide array of precision scientific applications, including quantum computing and communications [1–3], precision metrology [4], and optical atomic clocks [5]. Reducing the size, cost, weight, power consumption, and environmental sensitivity of these systems through photonic integration will open vast new application avenues, including space-based quantum and atomic systems [5] ultralow phase noise microwave sources [6], and energy-efficient high-capacity coherent communications [7]. In addition, the next generation atomic, molecular, and optical (AMO) [8] infrastructure will benefit from the ability to bring low losses, efficient lasers, and increasingly complex optical systems to the chip-scale for next generation applications, including example quantum computing [9], sensing [10], and molecular physics [8].

These precision applications rely on low optical phase noise and losses that, today, are delivered by free-space bulk optics [9] and table-top reference cavities with  $Q$  values of tens of billions [4]. While there has been progress in realizing compact bulk-optic and hybrid integrated resonators [11–14], translating this performance to wafer-scale (200 mm), CMOS-foundry-compatible solutions that approach a billion  $Q$  and 0.025 dB/m loss has remained elusive. Prior works in silicon nitride resonators include 422 million intrinsic  $Q$  and 0.060 dB/m waveguide loss [15] and  $Q$  values below 250 million [16,17]. Brillouin lasers have been demonstrated in near infrared wavelengths as well as visible [16,18–20], and a low lasing threshold is critical to energy efficiency and motivates further linewidth narrowing by higher order Stokes suppression [21]. Therefore, further reduction in waveguide loss, increased resonator  $Q$ , decreased linewidth, and lower optical thresholds for ultralow noise lasers are critical for energy efficiency and weight sensitive applications. Such waveguides and resonators will play an important role in quantum photonic circuits [22], precision spectral filtering for applications such as nonlinear quantum optics [3], and microwave synthesis using optical frequency division [6].

In this paper, we report a significant breakthrough in ultralow-loss and ultrahigh- $Q$  waveguide technology fabricated in a 200-mm wafer-scale, silicon nitride ( $\text{Si}_3\text{N}_4$ ) CMOS-foundry-compatible platform. We demonstrate 0.034 dB/m waveguide loss and a 720 million intrinsic  $Q$  resonator with 258 kHz intrinsic and 386 kHz loaded linewidths. These losses and linewidths are the lowest reported to date for a fully planar deposition, wafer-scale waveguide process, to the best of our knowledge. In addition, we show that these resonators can realize energy-efficient stimulated Brillouin scattering (SBS) lasing with a 380  $\mu$ W optical pump threshold power, and such lasers have been shown to demonstrate ultra-narrow linewidths [16]. This level of performance is achieved with a high-aspect-ratio TM mode  $\text{Si}_3\text{N}_4$  waveguide design combined with a nitride

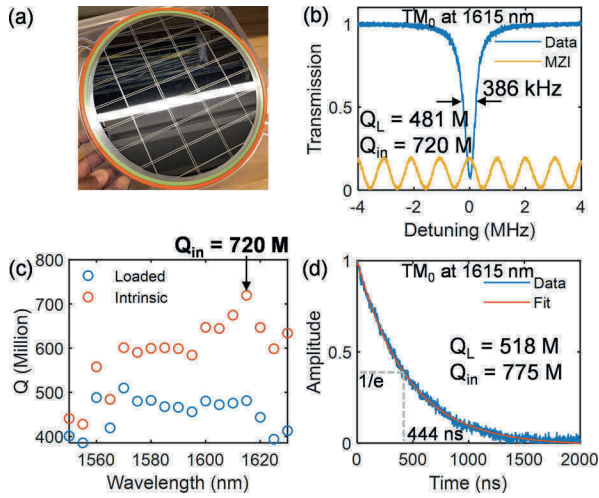


**Fig. 1.** Resonator linewidth and  $Q$ : (a) 200-mm wafer after the fabrication and dicing process; (b) resonance spectral scan at 1615 nm with the 1.078 MHz FSR MZI; (c) measured loaded and intrinsic  $Q$  values from 1550 nm to 1630 nm, where  $M$  = million; (d) a ringdown time of 444 ns, corresponding to an intrinsic  $Q = 775 M$  is measured at 1615 nm.

blanket layer and extra annealing steps to mitigate scattering and absorption losses [15]. These results show promise towards wafer-scale, manufacturable, ultralow-loss waveguides, ultrahigh- $Q$  resonators, and low threshold SBS lasers that today are achieved with bulk optics, bringing precision laser applications to the chip-scale and enabling a wide range of portable light sources and photonic circuits.

The resonator is a bus-coupled  $TM_0$  mode design with an 11  $\mu\text{m}$  wide by 80 nm thick silicon nitride core design and  $\sim 5$  nm blanket nitride layer located between a 15  $\mu\text{m}$  thick thermal oxide lower cladding and 6  $\mu\text{m}$  thick deposited upper cladding [15] fabricated on a 200 mm wafer-scale process [see Fig. 1(a)]. The 11.787 mm resonator radius is designed for SBS phase matching [16] while maintaining the bending losses to be relatively negligible (simulated to be  $<0.01$  dB/m). Our resonator design is guided by scattering loss simulation, based on a fully three-dimensional waveguide scattering loss model [23], which shows the  $TM_0$  mode scattering loss is much lower than that of the  $TE_0$  mode under the same waveguide roughness condition (see Supplement 1 for details on scattering loss modeling). We increased the core thickness to 80 nm to support the  $TM_0$  mode as well as the  $TE$  modes. The 6.898  $\mu\text{m}$  bus-ring coupling gap achieves slight under-coupling of the  $TM_0$  and very weak coupling of the  $TE$  modes (see Supplement 1 for bus-ring coupling simulation). Therefore, only the  $TM_0$  mode is properly coupled, and this coupling design makes it a quasi-single-mode resonator, although the waveguide by its nature is a multi-mode waveguide.

The loaded and intrinsic  $Q$  values are measured using a laser that tunes from 1550 nm to 1630 nm (Velocity TLB-6700), with a measured maximum of 720 million at 1615 nm, corresponding to a propagation loss of 0.034 dB/m. An intrinsic linewidth of 258 kHz and a loaded linewidth of 386 kHz [Figs. 1(b) and 1(c)] are measured using Mach-Zehnder interferometer (MZI) and ringdown techniques [15]. Ringdown measurements at 1615 nm yield an intrinsic  $775 \pm 8$  million and loaded  $518 \pm 5$  million  $Q$  [Fig. 1(d)], confirming the MZI measurement within 7%. The  $Q$

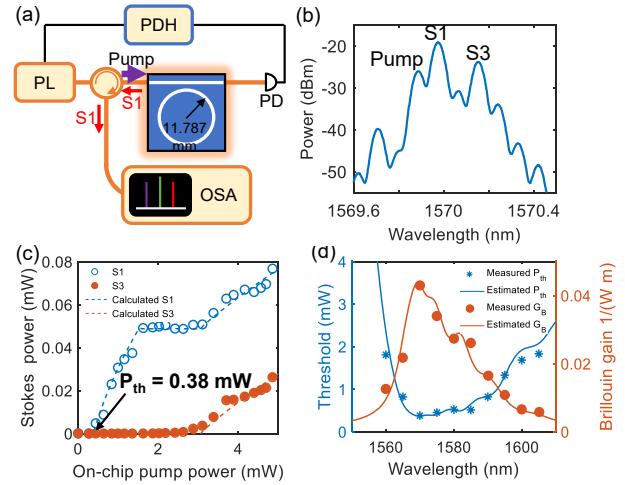


**Fig. 2.** SBS laser and threshold power measurement. (a) Setup for the SBS laser. PL, pump laser; PDH, Pound-Drever-Hall laser lock; PD, photodetector; OSA, optical spectrum analyzer. (b) Stokes power on the OSA with  $\sim 4$  mW on-chip pump power. (c) Measured S1 and S3 on-chip power with the calculated curves shows a threshold of 0.38 mW. (d) Calculated and measured threshold power and Brillouin gain from 1550 nm to 1610 nm.

and linewidth measurements at 1615 nm, of all 19 devices fabricated on the same 200 mm wafer, yield a maximum 720 million  $Q$  and average 565 million  $Q$  [see Fig. S1(a) in Supplement 1].

Next, we demonstrate a 380  $\mu\text{W}$  threshold for the first order Stokes (S1) Brillouin lasing operating at 1570 nm. A tunable laser (Velocity TLB-6700) is locked to the resonator using the Pound-Drever-Hall technique [24]. Measurement of S1 on an optical spectrum analyzer (OSA) [Fig. 2(b)] as a function of input pump power at 1570 nm [Fig. 2(c)] indicates a clear S1 threshold and a threshold power of 380  $\mu\text{W}$ . Similarly, the S1 threshold power is also measured at other wavelengths, shown in Fig. 2(d), indicating the 380  $\mu\text{W}$  threshold power at 1570 nm is the minimum threshold and the Brillouin gain at 1570 nm is at its maximum. Using the cascaded Brillouin laser model [25], we can simulate the S1 and S3 Stokes power [dashed curves in Fig. 2(c)] with the measured loaded and intrinsic  $Q$  at 1570 nm and an estimated Brillouin gain of  $0.043 (\text{m} \cdot \text{W})^{-1}$ . The laser power conversion efficiency for S1 at its first clamping point with the pump power of 1.5 mW is  $\sim 3.1\%$ . The low conversion efficiency is due to the bus-ring under-coupling ( $\gamma_c/\gamma_{in} \sim 0.17$ ). In the future, we plan to design the bus-ring coupling to have the resonator slightly over-coupled ( $\gamma_c/\gamma_{in} \sim 2$ ) so that the conversion efficiency can be dramatically increased without much increase in threshold [see Fig. S2(d) in Supplement 1]. Although SBS lasing implies potentially significant linewidth narrowing and ultra-narrow linewidth emission, it is the low conversion efficiency and lower output Stokes power that prevent us from carrying out any meaningful SBS laser frequency noise or linewidth measurements.

Each optical wavelength corresponds to a distinct phonon mode, where the phonon frequency depends on the optical frequency and acoustic speed,  $\Omega_B = 4\pi n V_{ac}/\lambda$ . Without the resonator, any wavelength of light can mediate SBS through an appropriately phase-matched phonon, while in the resonator, only resonator modes at wavelengths offset from the pump by the Brillouin frequency shift can mediate SBS. Therefore, in

addition to resonator  $Q$ , phase matching between the SBS frequency shift and integer multiple of the resonator free spectral range (FSR) are important in lowering the SBS threshold.

The SBS laser threshold is determined by the following equation [25]:

$$P_{th} = \frac{\pi^2 n_g^2 L Q_c}{G_B \lambda^2 Q_L^3},$$

where  $n_g$  is the group index,  $\lambda$  is the wavelength,  $Q_L(Q_c)$  is the loaded (bus-ring coupling)  $Q$  factor, and  $G_B$  is the waveguide Brillouin gain. The waveguide Brillouin gain in the waveguide resonator,  $G_B(\Delta\omega - \Omega_B)$ , is a function of both pump-Stokes frequency difference  $\Delta\omega = 4 \times \text{FSR}$  and the Brillouin shift frequency  $\Omega_B = 4\pi n V_{ac}/\lambda$ . With the measured  $Q$  values and S1 threshold, the resonator's Brillouin gain at different wavelengths can be calculated using the equation above, shown as solid circles in Fig. 2(d), where reaching a maximum Brillouin gain at 1570 nm indicates a good SBS phase matching at 1570 nm, thus  $\Delta\omega = \Omega_B$  and  $G_B(\Delta\omega - \Omega_B = 0) = 0.043 \text{ (m} \cdot \text{W)}^{-1}$ . Besides, the pump-S1 beatnote frequency at 1570 nm measured on an electric spectral analyzer (Fig. S2(b) in Supplement 1) indicates  $\Delta\omega = \Omega_B = 10.831 \text{ GHz}$ . The waveguide Brillouin gain spectrum simulated by COMSOL (Fig. S2(a) in Supplement 1) has a bandwidth of  $\sim 150 \text{ MHz}$  and is calibrated with a gain peak of  $0.043 \text{ (m} \cdot \text{W)}^{-1}$  at  $10.831 \text{ GHz}$ . While the FSR and index measured by the pump-S1 beatnote frequency stay fairly constant across the wavelength range (Fig. S2(b) in Supplement 1), the Brillouin shift frequency ( $\Omega_B = 4\pi n V_{ac}/\lambda$ ) change from the wavelength change is the major factor in the phase matching condition ( $\Delta\omega - \Omega_B$ ) and the Brillouin gain  $G_B(\Delta\omega - \Omega_B)$ , meaning that the  $150 \text{ MHz}$  Brillouin gain spectrum bandwidth corresponds to a gain window in the wavelength range of  $\frac{150 \text{ MHz}}{10.831 \text{ GHz}} \times 1570 \text{ nm} = 22 \text{ nm}$  [see Fig. S2(c) in Supplement 1]. By calculating the Brillouin shift frequency  $\Omega_B$  and using the simulated Brillouin gain spectrum, we can calculate the Brillouin gain as a function of wavelength (solid curve connecting solid circles in Fig. 2(d)), indicating good agreement between the calculated and measured values across this wavelength range. See Supplement 1 for details on the waveguide Brillouin gain spectrum simulation and SBS laser phase matching condition.

In conclusion, we demonstrate that  $0.034 \text{ dB/m}$  waveguide loss can be realized in a  $200 \text{ mm}$  wafer-scale CMOS-foundry-compatible silicon nitride process. Leveraging these low losses, we realize a  $720$  million intrinsic  $Q$  resonator with corresponding  $258 \text{ kHz}$  intrinsic and  $386 \text{ kHz}$  loaded linewidths. Finally, used as a nonlinear resonator, we demonstrate SBS lasing with a  $380 \text{ } \mu\text{W}$  threshold power. Further loss reduction is possible using techniques such as inverse pattern etching and reflow and optimization of TM mode waveguide geometries. Our investigation of the Brillouin gain and threshold shows a strong Brillouin phase matching at  $1570 \text{ nm}$ . The SBS laser conversion efficiency and threshold can be further improved in future work by optimizing the bus-to-ring coupling design and by changing the resonator FSR to phase match to wavelengths associated with higher  $Q$ , such as  $1615 \text{ nm}$ . These results demonstrate for the first time that this level of performance can be realized using fully planar, CMOS-compatible wafer-scale ( $200 \text{ mm}$ ) processes, without complex bonding or sidewall etch post processing. Moving forward, these results demonstrate the ability to bring table-top loss performance, ultrahigh- $Q$  filtering, and ultra-narrow linewidths to the chip-scale, as well as sub-mW lasing thresholds suitable for compact and low-power consumption

solutions for precision applications such as quantum, microwave, and atomic sensing.

**Funding.** Advanced Research Projects Agency - Energy (DE-AR0001042).

**Acknowledgment.** We thank Jiawei Wang for dicing the resonators and Mark Harrington for helpful discussions.

**Disclosures.** The authors declare no conflicts of interest.

**Data availability.** Data underlying the results presented in this paper are not publicly available at this time but may be obtained from the authors upon reasonable request.

**Supplemental document.** See Supplement 1 for supporting content.

## REFERENCES

1. A. Orieux and E. Diamanti, *J. Opt.* **18**, 083002 (2016).
2. H. Yonezawa, D. Nakane, T. A. Wheatley, K. Iwasawa, S. Takeda, H. Arao, K. Ohki, K. Tsumura, D. W. Berry, T. C. Ralph, H. M. Wiseman, E. H. Huntington, and A. Furusawa, *Science* **337**, 1514 (2012).
3. G. Zhang, J. Y. Haw, H. Cai, F. Xu, S. M. Assad, J. F. Fitzsimons, X. Zhou, Y. Zhang, S. Yu, J. Wu, W. Ser, L. C. Kwek, and A. Q. Liu, *Nat. Photonics* **13**, 839 (2019).
4. D. G. Matei, T. Legero, S. Häfner, C. Grebing, R. Weyrich, W. Zhang, L. Sonderhouse, J. M. Robinson, J. Ye, F. Riehle, and U. Sterr, *Phys. Rev. Lett.* **118**, 263202 (2017).
5. A. D. Ludlow, M. M. Boyd, J. Ye, E. Peik, and P. O. Schmidt, *Rev. Mod. Phys.* **87**, 637 (2015).
6. J. Li, H. Lee, and K. J. Vahala, *Nat. Commun.* **4**, 2097 (2013).
7. D. J. Blumenthal, H. Ballani, R. O. Behunin, J. E. Bowers, P. Costa, D. Lenoski, P. A. Morton, S. Papp, and P. T. Rakich, *J. Lightwave Technol.* **38**, 3376 (2020).
8. J. L. Bohn, A. M. Rey, and J. Ye, *Science* **357**, 1002 (2017).
9. H.-S. Zhong, H. Wang, and Y.-H. Deng, *et al.*, *Science* **370**, 6523 (2020).
10. C. Xu, L. Zhang, S. Huang, T. Ma, F. Liu, H. Yonezawa, Y. Zhang, and M. Xiao, *Photonics Res.* **7**, A14 (2019).
11. I. S. Grudinin, V. S. Ilchenko, and L. Maleki, *Phys. Rev. A* **74**, 063806 (2006).
12. W. Zhang, L. Stern, D. Carlson, D. Bopp, Z. Newman, S. Kang, J. Kitching, and S. B. Papp, *Laser Photonics Rev.* **14**, 1900293 (2020).
13. J. P. Hendrie, N. Jin, P. Kharel, F. Quinlan, P. Rakich, and S. A. Diddams, in *Conference on Lasers and Electro-Optics* (Optical Society of America, 2021), paperSTh4J.2.
14. L. Wu, H. Wang, Q. Yang, Q. Ji, B. Shen, C. Bao, M. Gao, and K. Vahala, *Opt. Lett.* **45**, 5129 (2020).
15. M. W. Puckett, K. Liu, N. Chauhan, Q. Zhao, N. Jin, H. Cheng, J. Wu, R. O. Behunin, P. T. Rakich, K. D. Nelson, and D. J. Blumenthal, *Nat. Commun.* **12**, 934 (2021).
16. S. Gundavarapu, G. M. Brodnik, M. Puckett, T. Huffman, D. Bose, R. Behunin, J. Wu, T. Qiu, C. Pinho, N. Chauhan, J. Nohava, P. T. Rakich, K. D. Nelson, M. Salit, and D. J. Blumenthal, *Nat. Photonics* **13**, 60 (2018).
17. D. T. Spencer, J. F. Bauters, M. J. R. Heck, and J. E. Bowers, *Optica* **1**, 153 (2014).
18. H. Lee, T. Chen, J. Li, K. Y. Yang, S. Jeon, O. Painter, and K. J. Vahala, *Nat. Photonics* **6**, 369 (2012).
19. K. Liu, M. W. Puckett, M. W. Harrington, G. M. Brodnik, Q. Zhao, N. Chauhan, J. Wang, R. O. Behunin, K. D. Nelson, and D. J. Blumenthal, in *CLEO* (2021).
20. N. Chauhan, A. Isichenko, K. Liu, J. Wang, Q. Zhao, R. O. Behunin, P. T. Rakich, A. M. Jayich, C. Fertig, C. W. Hoyt, and D. J. Blumenthal, *Nat. Commun.* **12**, 4685 (2021).
21. H. Wang, L. Wu, Z. Yuan, and K. Vahala, "Towards milli-Hertz laser frequency noise on a chip," arXiv:2010.09248 [physics] (2020).
22. A. W. Elshaari, W. Pernice, K. Srinivasan, O. Benson, and V. Zwiller, *Nat. Photonics* **14**, 285 (2020).
23. C. Ciminelli, F. Dell'Olio, V. M. N. Passaro, and M. N. Armenise, *Opt. Quantum Electron.* **41**, 285 (2009).

24. E. D. Black, *Am. J. Phys.* **69**, 79 (2001).
25. R. O. Behunin, N. T. Otterstrom, P. T. Rakich, S. Gundavarapu, and D. J. Blumenthal, *Phys. Rev. A* **98**, 023832 (2018).